http://dx.doi.org/10.5012/bkcs.2013.34.8.2291

Carbon Monoxide Sensor Based on a B2HDDT-doped PEDOT:PSS Layer

R. Memarzadeh,[†,#,a] Hui-Bog Noh,[#,a] S. Javadpour,[†,*] F. Panahi,[‡] A. Feizpour,[§] and Yoon-Bo Shim[#,*]

[†]*Department of Materials Science & Engineering, Shiraz University, Shiraz, Iran.* [*]*E-mail: sirus.javadpour@gmail.com*
[‡]*Department of Chemistry, College of Sciences, Shiraz University, Shiraz, Iran*
[§]*Department of Chemistry and the Photonics Center, Boston University, Boston, Massachusetts 02215, U.S.A.*
[#]*Department of Chemistry and Institute of BioPhysio Sensor Technology, Pusan National University, Busan 609-735, Korea*
[*]*E-mail: ybshim@pusan.ac.kr*
Received April 24, 2013, Accepted May 7, 2013

An efficient carbon monoxide (CO) sensor was developed based on poly(3,4-ethylenedioxy)thiophene-poly(styrenesulfonate) (PEDOT:PSS) modified with a new pyrimidine-fused heterocyclic compound, bis(2-hydroxyphenyl)dihydropyrido[2,3-*d*:6,5-*d*]dipyrimidine-tetraone (B2HDDT). B2HDDT remains stable in the polymer matrix through interactions with functional groups of the polymer. It created prominent sites that captured CO gas, and the experimental parameters, including the amount of doped B2HDDT in the PEDOT:PSS film, were optimized. The sensor probe was also examined to verify its reliability for detecting CO in the presence of atmospheric gases in a discriminating manner. NMR, AFM, and FT-IR spectra were obtained to evaluate the structure and morphology of the B2HDDT-doped PEDOT:PSS (PEDOT:PSS/B2HDDT) film. The content of 35 vol % B2HDDT (7.0 mM) in PEDOT:PSS provided the largest response factor ($\Delta R/R_o$) for the CO gas. The sensor response was reproducible, with a relative standard deviation < 5% (n = 5). The detection limit was determined to be 0.44 ± 0.05 vol %.

Key Words : PEDOT:PSS, Gas sensor, Carbon monoxide, Conductive polymer

Introduction

Carbon monoxide (CO) is an odorless and colorless gas, which makes it a well-known silent killer. Monitoring of the CO concentration in air is therefore necessary. The conventional materials used for CO sensors are semiconducting metal oxides, solid electrolytes, and ionic membranes. In addition to these materials, conducting polymers have been used for this application.[1] Until now, polyanilines, polypyrroles, polythiophenes, and their derivatives have been successfully used for CO sensing. They have the advantages of low cost, low temperature requirements, and ease of fabrication compared with other materials used to detect CO. Moreover, conducting polymers have other desirable properties, such as piezoresistivity, spectral sensitivity (an increase in resistance under irradiation by photons of different wavelengths), and thermistors properties.[2]

Among the conducting polymers, poly(3,4-ethylenedioxy)thiophene (PEDOT) composite is one of the materials used for sensor fabrication. Dispersion of PEDOT and poly(styrenesulfonate) (PSS) in water has been used in diverse sensor applications in recent years.[3] In addition, PEDOT:PSS has also been doped with other compounds, such as dimethyl sulfoxide, tetrahydrofuran (THF), sorbitol, 2-nitroethanol, methyl sulfoxide, polyethylene glycol, and ethylene glycol, to increase its conductivity (100-fold in some cases), which can change the sensing properties of the polymers.[4] This strategy has also been utilized to great benefit in the biomedical field for biosensing and drug delivery applications.[5] A PEDOT:PSS/nanotube composite has been used in a controlled drug release system.[6] PEDOT:PSS/Au nanocomposites and inkjet-printed PEDOT:PSS have been used as new transducers with enzyme immobilization in amperometric glucose biosensors.[7] PEDOT:PSS has recently attracted significant attention for its applications in gas sensors: PEDOT:PSS nanocomposites, PEDOT:PSS/Pd and PEDOT:PSS/polyvinylpyrrolidone, were used as sensors for chemical vapors (ethanol, methanol, THF, and acetone) and NO and NH_3 gases.[8] The inclusion of dopant molecules into a conductive polymer is beneficial to sensor performance. For example, a metal complex and morphline were used as dopants for detection of CO.[9] Thus, we have investigated new dopant molecules to enhance sensor performance.

In the present study, an efficient PEDOT:PSS-based CO sensor was studied through modification of PEDOT:PSS with a new pyrimidine-fused heterocyclic compound, bis(2-hydroxyphenyl)dihydropyrido[2,3-*d*:6,5-*d*]dipyrimidine-tetraone (B2HDDT). This doping molecular dopant contains numerous functional groups that produce hydrogen bonds with target molecules and with the polymer matrix.[10] Therefore, this compound can be used as a dopant in PEDOT:PSS to improve the properties of the polymer for CO detection. Hence, B2HDDT-doped PEDOT:PSS was investigated for its ability to detect CO in the atmosphere.

Experimental

Materials and Interdigitate Electrodes. Chemicals were

[a]These authors contributed equally to this work.

purchased from Fluka and Sigma-Aldrich (U.S.A.) and used without further purification. CO, N_2, CO_2, and O_2 gases were used as received from P. S. Chem (S. Korea). PEDOT:PSS was used as received from Sigma-Aldrich (U.S.A.) in a blue colloidal suspension in water. This polymer suspension contained 1.0 wt % solid content and exhibited a maximum viscosity of 15 mPa·s and a surface resistance of 20 MΩ. An Au-interdigitate electrode was produced as a microelectromechanical system that consisted of an Au layer with a thickness of 25.0 nm and an effective area of 4.0 mm × 5.0 mm deposited on a silicon wafer with a die size of 12.0 mm × 11.0 mm. The width of the Au electrodes was 8.0 μm, and equidistant gaps of 6.0 μm were left between each electrode. The conducting polymer was spin-coated onto the interdigitate electrode.

Characterization and Measurements. Nuclear magnetic resonance (NMR) spectra were recorded on a Bruker Avance 250 MHz spectrometer. A solution of the complex in $CDCl_3$ was prepared using tetramethylsilane (TMS) as the internal standard. Fourier-transform infrared (FT-IR) spectroscopy (Shimadzu FT-IR 8300 spectrophotometer) was used to characterize the materials. Melting-points were determined using open capillary tubes in a Barnstead Electro-thermal 9100 BZ circulating oil melting point apparatus. The synthesis reaction was monitored by TLC on PolyGram SILG/UV254 silica-gel plates. Column chromatography was performed using silica gel 60 (70-230 mesh). Atomic force microscopy (AFM) image was obtained on a Digital Instrument Nanoscope™ 3D ADC5, Multi-mode (Veeco Instruments Inc., CA) operated in a tapping mode.

Bare interdigitate Au electrodes were washed with distilled water and cleaned using an ultrasonic cleaner. Each electrode was cleaned with acetone, dried, and then coated with the polymer. Different compositions of the doped polymer were cast onto the top of the substrates at 1200 rpm for 5 sec. The prepared sensor probe was subsequently placed in a chamber with a controlled atmosphere, wherein the gas inlet and outlet pressure could be measured and controlled. An electrometer/high resistance meter (Keithley, CIMS model 6517A, U.S.A.) was used to monitor the variations in the resistance of the thin films. The ratio of the gas mixture was controlled using precision gas flow meters (KOFLOC, Model RK1200, Japan).

Synthesis of Bis(2-hydroxyphenyl)dihydropyrido[2,3-*d*:6,5-*d*]dipyrimidine-tetraone (B2HDDT). A pseudo-four-component coupling reaction between barbituric acid (**1**), amine, and benzaldehyde was performed to synthesize the dihydropyrido[2,3-*d*:6,5-*d*]dipyrimidine-tetraone derivative. These reagents were produced in almost quantitative yields. The bis(2-hydroxyphenyl)dihydropyrido[2,3-*d*:6,5-*d*]dipyrimidine-tetraone (**4**; B2HDDT) was synthesized using a multicomponent coupling reaction between barbituric acid, 2-aminophenol (**2**) and 2-hydroxybenzaldehyde (**3**) (Scheme 1).

A mixture of barbituric acid (0.26 g, 2.0 mmol), 2-hydroxybenzaldehyde (0.11 g, 1.0 mmol), 2-aminophenol (0.12 g, 1.0 mmol), and *p*-toluene sulfonic acid (PTSA) (0.1 g, 58.0 mol %) in refluxing ethanol (5.0 mL) was stirred for 4 h. After the reaction was complete, as confirmed by TLC (eluent: EtOAc/*n*-hexane), the reaction mixture was cooled to room temperature. The precipitated product was subsequently filtered and washed with water (20.0 mL) and ethanol (10.0 mL) to give the pure product as a yellow powder (0.395 g, 91%): IR (KBr): ν = 3114, 2638, 2383, 1728, 1630, 1519, 1352, 1124, 858, 787, 785, and 555 cm^{-1}. ^1H NMR (250 MHz, DMSO/TMS) δ 4.25 (s, 1H), 6.88 (q, *J* = 6.6, 2.1 Hz, 1H), 7.03 (d, *J* = 8.3 Hz, 1H), 7.17-7.28 (m, 3H), 7.49 (d, *J* = 6.3, 1H), 7.66 (d, *J* = 8.8, 2H), 8.04 (brs, 2H), 10.28 (brs, 1H), and 10.62 (brs, 1H). ^{13}C NMR (62.9 MHz, DMSO/TMS) δ 35.1, 80.3, 115.5, 116.8, 117.9, 121.2, 1217, 122.5, 122.8, 127.4, 130.1, 144.0, 152.2, 152.7, 157.0, and 165.1. Anal. Calcd for $C_{21}H_{15}N_5O_6$ (433.1): C, 58.20; H, 3.49; N, 16.16. Found: C, 58.12; H, 3.41; N, 16.06.

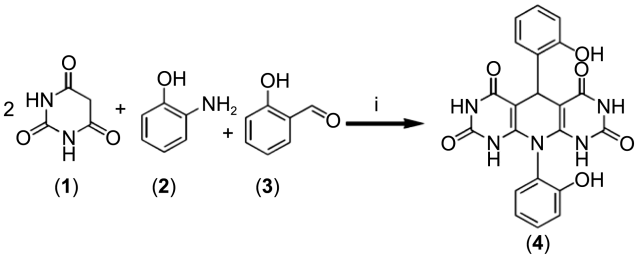

Scheme 1. The multi-component method for the synthesis of B2HDDT. i) PTSA, ethanol, and reflux for 4 h.

Table 1. Four different compositions of B2HDDT in PEDOT:PSS

Compositions	PEDOT:PSS dispersion (vol %)	B2HDDT solution (vol %)
P3B1	75	25
P2B1	65	35
P1B1	50	50
P1B2	35	65

Doping Procedure. The PEDOT:PSS was doped with a solution of B2HDDT (7.0 mL) with four different volume fractions, as shown in Table 1. To obtain a homogenous mixture in water, the mixing solution was stirred for 6 hrs to allow compounds to interact thoroughly with the polymer.

Results and Discussion

Gas-sensing Properties. The responses of the PEDOT:PSS thin film, which was doped with 35 vol % aqueous B2HDDT (P2B1), to O_2, N_2, CO, and CO_2 were evaluated, where each gas flowed in a vacuum chamber at a rate of 17.0 mL/min. Figure 1 shows the different percentage in the resistance of the sensing probe according to the test gases.

$$S = (R_{thf} - R_o)/R_o \quad (1)$$

where S is the sensor probe response, R_{thf} is the measured thin-film resistance for different gases, and R_o is the thin film resistance under the initial vacuum state. Therefore, a high value of $|S|$ indicated a high response for each gas,

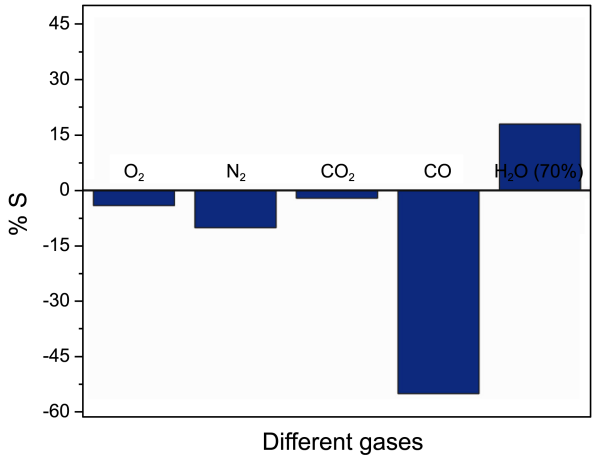

Figure 1. Response of the P2B1 composite to common gases in the atmosphere.

although more sophisticated experiments were required in which the sensor probe was exposed to the mixture of air and CO. The results show that the sensor exhibits the highest response to CO, whereas it exhibited small responses toward the other gases, as shown in Figure 1. Since the PEDOT:PSS has a polar structure, it can easily retain moisture; therefore, the contamination of the sensor by moisture in the atmosphere results in small change in resistance. In practice, the desired vacuum pressure might not be fully achieved in the experiment chamber. Therefore, it is possible that the nitrogen flowing over the sensor did not entirely eliminate the moisture trapped on the sensor surface and therefore resulted in a small decrease in the sensor resistance under the N_2 atmosphere. To minimize this effect, silicate was used inside the testing chamber. Some studies have indicated that gases with polar molecules, such as H_2O and CO can affect the resistivity of conducting polymers with that chain structures.[8c,11] Therefore, we postulate that air is one of the gases that interferes with the measurements performed using PEDOT:PSS-based sensors because it contains a constant partial pressure of water vapor. The other common gases in air were not observed to significantly affect this polymer sensor.

The effect of air on the sensor response was investigated and plotted as a function of time (sec). The temperature and relative humidity were approximately 24 °C and 70%, respectively. As shown in Figure 2(a), the resistance of the doped and undoped PEDOT:PSS changed in the presence of air. The film resistance decreased in air with respect to that measured in the vacuum background. The response of the PEDOT:PSS probe doped with B2HDDT in air, which contains water vapor, decreased compared to that of the undoped polymer. When the B2HDDT content increased, the effect was enhanced. Furthermore, the response time was short, and the sensor reached its maximum response within 5 sec; the short response time is one of the most important characteristics of this polymer sensor. The resistance of the undoped and doped PEDOT:PSS decreased after the polymer was exposed to carbon monoxide and showed a negative

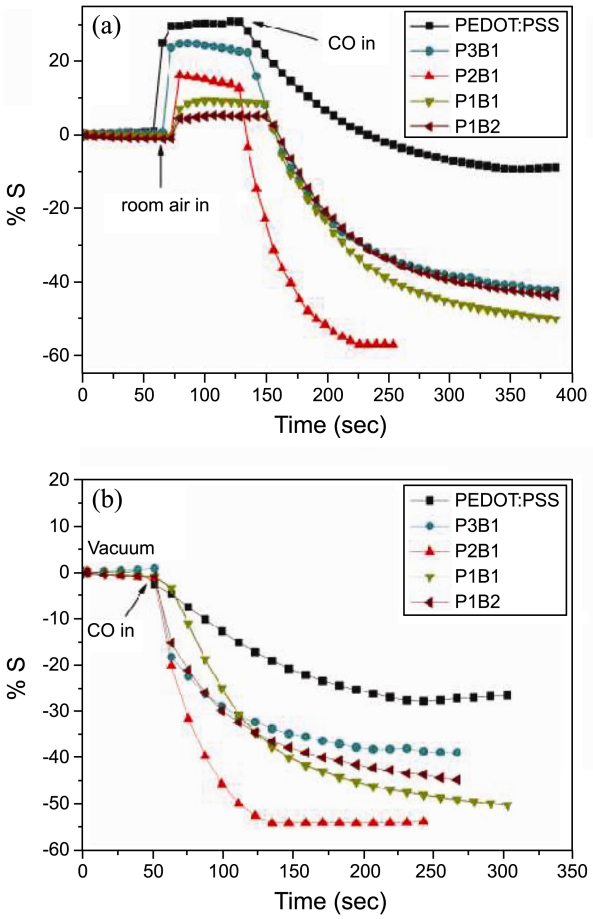

Figure 2. (a) Response curves obtained for PEDOT:PSS and four different compositions of B2HDDT-doped PEDOT:PSS under exposure to CO while the chamber was filled with air. (b) Response curves for PEDOT:PSS and four different compositions of B2HDDT-doped PEDOT:PSS under exposure to CO in an evacuated chamber. (Flow rate of CO = 17.0 mL/min, temperature = 24 °C, and relative humidity = 70%).

response because the reaction with CO proceeded in the reverse direction relative to the reaction with air. Among the four concentrations that were tested, sample P2B1 showed the largest response value, which was approximately -55%; this response represented a significant improvement in response.

The sensor response to CO under vacuum was also investigated, as shown in Figure 2(b), where the sensor composed of different compositions of PEDOT:PSS and B2HDDT was examined by the saturation of CO in an evacuated chamber. The higher response of P1B1 in comparison with that of P1B2 shows that the effect of the B2HDDT concentration on the CO response is not linear. The P2B1 composition in doped PEDOT:PSS exhibited the greatest response to the CO gas, which demonstrates that this composition is the best candidate for a CO sensor. This composition exhibited a significantly better response value than did the compositions reported in our recent work, where morpholine was used as a dopant.[9b]

The reproducibility of PEDOT:PSS-based sensors was

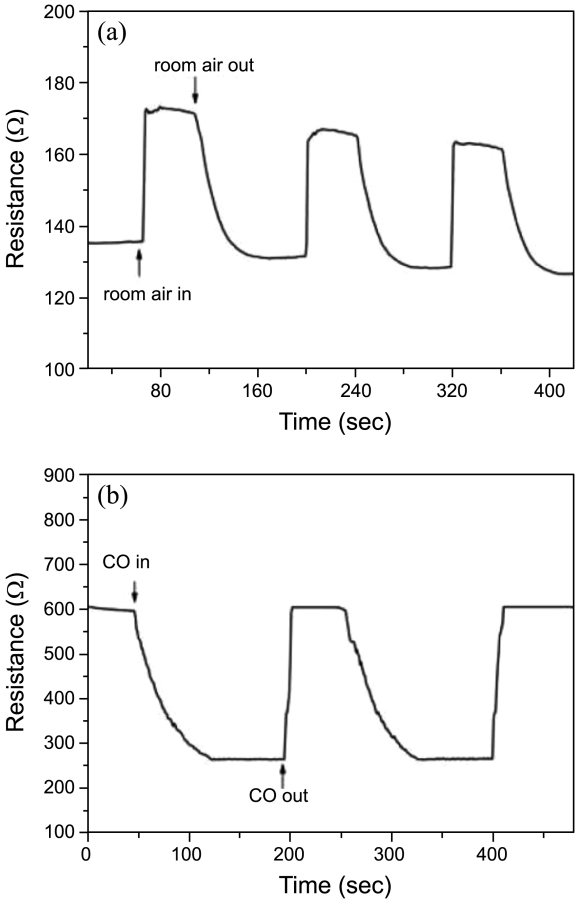

Figure 3. Reproducibility of doped PEDOT:PSS (P2B1): (a) the effect of room air on the vacuum background and (b) the effect of CO gas in the room air background. (Flow rate of CO = 17.0 mL/min, temperature = 24 °C, and relative humidity = 70%).

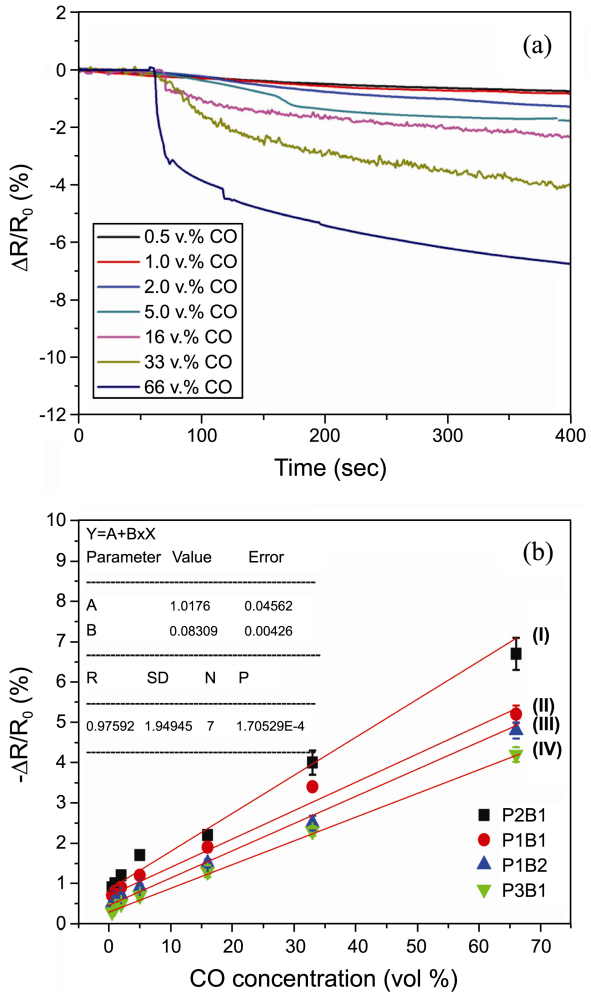

Figure 4. (a) Response of the P2B1 sensor to various concentrations of CO gas. (b) Calibration plot of the resistance responses of **(I)** P2B1, **(II)** P1B1, **(III)** P1B2, and **(IV)** P3B1 sensors versus the concentration of CO gas. (Flow rate of CO = 10.0 mL/min, temperature = 24 °C, and relative humidity = 70%).

also excellent. As shown in Figure 3(a), a doped PEDOT:PSS film exposed to air and then placed under vacuum exhibited a reproducible response. Figure 3(b) shows that the doped probe also exhibited a reproducible response for CO in the air background.

Figure 4(a) shows a typical resistance response of the sensor to the various concentrations of CO gas at room temperature (24 °C). The sensor resistance increased with increasing CO gas concentration. The data show that the sensor produced a 6.7% resistance change upon exposure to 66 vol % CO gas. An almost 0.9% variation in the resistance was observed even for the sensor with a CO gas concentration of only 0.5 vol %. The calibration curve was obtained by plotting the resistance change as a function of the sample concentration for all the sensor compositions (**(I)** P2B1, **(II)** P1B1, **(III)** P1B2, and **(IV)** P3B1) as shown in Figure 4(b), and the largest response was observed for the P2B1 sensor. In this case, the magnitude of the response was expressed as the $(-\Delta R/R_0)$ *vs.* concentration (vol %). The response magnitude of 0.092 ± 0.007 (vol %) was obtained from the slope of the calibration plot in the linear region, as shown in Figure 4(b). The correlation coefficient of 0.97592 demonstrates that the P2B1 sensor exhibits good linearity for CO.

From the calibration plot in Figure 4(b), the detection limit of the B2HDDT doped PEDOT:PSS sensor was determined according to Eqs. (2) and (3).[12]

$\text{Mean}_{\text{blank}} = 0.26$
$\text{SD}_{\text{blank}} = 0.068$
$\text{SD}_{\text{low concentration sample}} = 0.045$

according to the formula:

$$\text{B.L.} = \text{Mean}_{\text{blank}} + 1.645\ (\text{SD}_{\text{blank}}) = 0.37 \quad (2)$$
$$\text{D.L.} = \text{B.L.} + 1.949\ (\text{SD}_{\text{low concentration sample}}) = 0.46 \quad (3)$$

To estimate the B.L. (blank limit), the replicates of the blank samples were measured. The mean and standard deviation (SD) of the results were calculated.

AFM Image of Probe Polymer Film. Because P2B1 exhibited the best response toward CO, we representatively analyzed the polymer film of P2B1. Figure 5 shows the atomic force microscopic topology of the doped-polymer film (P2B1) formed on the sensor surface. The AFM image of the film shows the roughness, the uniformity of the film,

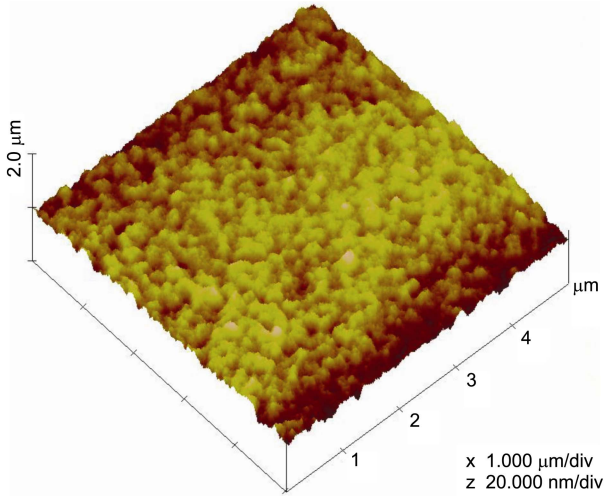

Figure 5. The AFM image of the surface of doped-PEDOT:PSS thin film (P2B1).

and its thickness. A highly uniform surface was obtained in this case: the root mean square value of the surface roughness was 0.732 nm. The thickness of the coated polymer layer was determined to be ~3.4 nm. This result indicates that the spin-coating procedure performed under the experimental conditions used in this study produced a homogenous surface without cracks, pores, or other types of defects. Therefore, the investigated thin film is ideal for use as a gas sensor because the uniformity of films produced by the spin-coating process is one of the key factors in the repeatability of gas-sensing experiments.

FT-IR Analysis of B2HDDT and the Doped Polymer. The FT-IR spectra of PEDOT:PSS (65 vol %) and PEDOT:PSS/B2HDDT (35 vol %) are shown in Figure 6(a). The absorption band shift observed in the absorption spectra after the detection of CO confirms an interaction between the CO (100%) gas and the polar functional groups in B2HDDT. A comparison between them also indicates the presence of B2HDDT in the structure of PEDOT:PSS. The differences between the FT-IR spectrum of PEDOT:PSS and that of PEDOT:PSS/B2HDDT layers reveal some specific absorption bands for B2HDDT. The FT-IR spectra of PEDOT:PSS/B2HDDT and PEDOT:PSS show bands at 1504, 1389, 1088, 814, and 743 cm^{-1}, which are presumably due to the bonds in PEDOT:PSS.[10b] In addition, the bands at approximately 1743 and 1643 cm^{-1} are related to the carbonyl group of the B2HDDT compound. The weak band at 2120 cm^{-1} is due to the stretching vibrations of the C-H and C-C bonds of B2HDDT. The appearance of this band indicates the presence of B2HDDT in the PEDOT:PSS layer. The small shifts observed in the absorption bands of PEDOT:PSS and B2HDDT are related to the interaction between them. Figure 6(b) shows the FT-IR spectra of B2HDDT **(I)** before and **(II)** after the interaction with CO. A comparison between the FT-IR spectra reveals a slight shift in the absorption bands of B2HDDT toward higher energy after the absorption of CO. This band shift confirms an interaction between the CO gas and the polar functional groups in B2HDDT.

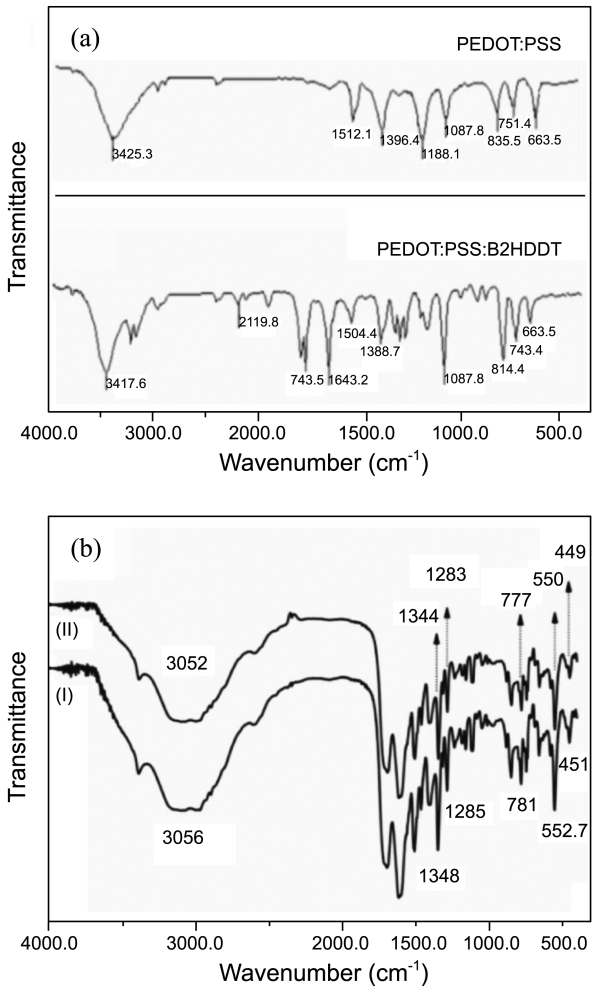

Figure 6. (a) FT-IR spectra of pure PEDOT:PSS and PEDOT:PSS/B2HDDT (P2B1), and (B) the B2HDDT molecule **(I)** before and **(II)** after the reaction with CO.

Conclusion

In the present study, an efficient and reversible carbon monoxide sensor based on the B2HDDT-doped PEDOT:PSS polymer was developed. The new compound B2HDDT, which was effective toward CO sensing, was synthesized using a single-step and multi-component reaction with relatively inexpensive starting materials. B2HDDT can form hydrogen bonds with the PEDOT:PSS polymer matrix, and it remains stable in the polymer structure. The interaction between CO and the B2HDDT-doped PEDOT/PSS is remarkably fast at room temperature. The PEDOT:PSS with the 35 vol % B2HDDT solution (7.0 mM) was the best-performing composition because it showed the largest response to CO gas in the atmosphere.

Acknowledgments. This work was supported by a 2-Year Research Grant of Pusan National University (South Korea).

References

1. (a) Adhikari, B.; Majumdar, S. *Prog. Polym. Sci.* **2004**, *29*, 699.

(b) Bai, H.; Shi, G. *Sensors* **2007**, *7*, 267. (c) Lange, U.; Roznyatovskaya, N. V.; Mirsky, V. M. *Anal. Chim. Acta* **2008**, *614*, 1. (d) Rahman, Md. A.; Kumar, P.; Park, D.-S Shim, Y.-B. *Sensors* **2008**, *8*, 118.
2. (a) Latessa, G.; Brunetti, F.; Reale, A.; Saggio, G.; Carlo, A. D. *Sens. Actuators B* **2009**, *139*, 304. (b) Kwon, I. W.; Son, H. J.; Kim, W. Y.; Lee, Y. S.; Lee, H. C. *Synth. Met.* **2009**, *159*, 1174.
3. Groenendaal, L.; Jonas, F.; Freitag, D.; Pielartzik, H.; Reynolds, J. R. *Adv. Matter.* **2000**, *2*, 481.
4. (a) Ouyang, J.; Xu, Q.; Chu, C.-W.; Yang, Y.; Li, G.; Shinar, J. *Polymer* **2004**, *45*, 8443. (b) Wang, T.; Qi, Y.; Xu, J.; Hu, X.; Chen, P. *Appl. Surf. Sci.* **2005**, *250*, 188.
5. Collazos-Castro, J. E.; Polo, J. L.; Hernandez-Labrado, G. R.; Padial-Canete, V.; Garcia-Rama, C. *Biomaterials* **2010**, *31*, 9244.
6. Abidian, M. R.; Kim, D.; Martin, D. *Adv. Mater.* **2006**, *18*, 405.
7. (a) Setti, L.; Fraleoni-Morgera, A.; Ballarin, B.; Filippini, A.; Frascaro, D.; Piana, C. *Biosens. Bioelectron.* **2005**, *20*, 2019. (b) Xu, J.; Peng, R.; Ran, K.; Xian, Y.; Tian, Y.; Jin, L. *Talanta* **2010**, *82*, 1511.
8. (a) Yin, K.; Zhu, Z. *Synth. Met.* **2010**, *160*, 1115. (b) Choi, J.; Lee, J.; Choi, J.; Jung, D.; Shim, S. E. *Synth. Met.* **2010**, *160*, 1415. (c) Lin, C.; Chen, J.; Hu, C.; Tunney, J. J.; Ho, K. *Sens. Actuators B* **2009**, *140*, 402.
9. (a) Memarzadeh, R.; Panahi, F.; Javadpour, S.; Khalafi-Nezhad, A.; Noh, H.-B.; Shim, Y.-B. *Bull. Korean Chem. Soc.* **2012**, *33*, 1297. (b) Javadpour, S.; Gharavi, A.; Feizpour, A.; Khanehzar, A.; Panahi, F. *Sens. Actuators B* **2009**, *142*, 152.
10. (a) Gangjee, A.; Adair, O. O.; Pagley, M.; Queener, S. F. *J. Med. Chem.* **2008**, *51*, 6195. (b) Chan, D. C. M.; Fu, H.; Forsch, R. A.; Queener, S. F.; Rosowsky, A. *J. Med. Chem.* **2005**, *48*, 4420. (c) Wamhoff, H.; Dzenis, J.; Hirota, K. *Adv. Heterocycl. Chem.* **1992**, *55*, 129.
11. Sotzing, G. A.; Briglin, S. M.; Grubbs, R. H.; Lewis, N. S. *Anal. Chem.* **2000**, *72*, 3181.
12. Armbruster, D. A.; Pry, T. *Clin. Biochem. Rev.* **2008**, *29*, S49.